Journal of Molecular Graphics and Modelling 44 (2013) 286–296

Contents lists available at ScienceDirect

Journal of Molecular Graphics and Modelling

journal homepage: www.elsevier.com/locate/JMGM

Insights from simulations into the mechanism of human topoisomerase I: Explanation for a seeming controversy in experiments

Neslihan Ucuncuoglu[a], Ioan Andricioaei[b], Levent Sari[a,c,*]

[a] Department of Physics, Fatih University, Istanbul 34500, Turkey
[b] Department of Chemistry, University of California, Irvine, CA 92697, United States
[c] Medical School, Fatih University, Istanbul 34500, Turkey

ARTICLE INFO

Article history:
Accepted 5 July 2013
Available online 24 July 2013

Keywords:
Human topoisomerase I
DNA supercoiling
Molecular dynamics
Force-field
Mutation

ABSTRACT

Human topoisomerase-I is a vital enzyme involved in cellular regulation of DNA supercoiling. We extend our previous work on wild type enzyme [13] to study how different enzyme mutants with various parts of the protein clamped by disulfide mutations affect DNA rotation. Three different mutants have been simulated; they are clamped enzyme-DNA systems in which the disulfide bridge is formed by replacing His367 and Ala499, Gly365 and Ser534, and, respectively, Leu429 and Lys436 with Cys pairs. The first of these mutants, a 'distally clamped' enzyme, mimics the experimental study of Carey et al. [11], which reports DNA rotation within the clamped enzyme. The second one, a 'proximal clamp', mimics the study of Woo et al. [12], who *do not* observe DNA rotation. The third is a newly suggested mutant that clamps the hinge for protein opening; we use it to test a hypothesis on negative supercoil relaxation. Our simulations show that the helical domain α5 totally melts in relaxation of positive supercoils when the enzyme is proximally clamped, while it preserves its structure very well within the distally clamped one. Moreover, a distally clamped protein permits DNA rotations in both directions, while the proximal clamp allows rotations only for *negatively* supercoiled DNA. These observations reconcile the two seemingly contradictory experimental findings, suggesting that subtle changes in the location of the disulfide bridge alter the mechanism significantly.

1. Introduction

Topoisomerases (topos) are enzymes that adjust the topology of DNA, with very important roles in replication [1], transcription [2], recombination [3,4], and repair [5]. They relieve supercoils, knots catenanes [6] generated during the genetic transactions in the cell [7,8]. These enzymes are classified as type I or type II, depending on whether they cleave one or both strands of the DNA. Type I topos are further subcategorized as type IA if the enzyme attaches to 5′ end of the DNA, or type IB if it the attachment happens to be with the 3′ end of the DNA.

Human topoisomerase I (a type IB topo) is a monomeric protein of 765 amino acids which is composed of four major regions [8,9]: a N-terminal, a core, a linker, and a C-terminal domain. As illustrated in Fig. 1, the core subdomain I (from Ile215 to Glu232 and from Ser320 to Ser433) and core subdomain II (from Pro233 to Met319) constitute an 'upper cap', which is connected by a flexible 'hinge' (a loop approximately from Leu429 to Lys436, between β11 and α8) to the bottom part of the clamp that has the C-terminal (Gln713 to Phe765) and the core subdomain III (Arg434 to Ala635). The linker domain is formed by an amino acid sequence from Pro636 to Lys712 (α18 and α19). The 'nose-cone' helices, α5 (Thr303 to Gln318) and α6 (Lys321 to Tyr338) that form a "V" shape structure believed to be important in the topoisomerization mechanism [10] belong to core subdomain II and I, respectively. The upper cap and the lower one interact via the 'lips' region opposite to the hinge side. The upper side of the lips is composed of a loop from core subdomain I, and the lower lip of two loops from core subdomain III. The protein is believed [10] to open up by parting the lips region to bind the DNA. Champoux et al. [9,10] provided two crystal structures, pdb codes 1A31 and 1A36. In one of them (pdb code 1A31), the protein is missing the non-essential N-terminal part (the first 214 residues), the linker (residues 636–712), 627–659 of the core and 713–719 of the C-terminal domains, and is covalently bound to a 22 base pair DNA duplex. In the other one (pdb code 1A36), the protein has the full amino acid sequence except the N-terminal part and 634–640 of the core, and bounds to DNA non-covalently.

* Corresponding author at: Medical School, Fatih University, Istanbul 34500, Turkey. Tel.: +90 2128663300.
E-mail address: lsari@fatih.edu.tr (L. Sari).

1093-3263/$ – see front matter © 2013 Elsevier Inc. All rights reserved.
http://dx.doi.org/10.1016/j.jmgm.2013.07.003

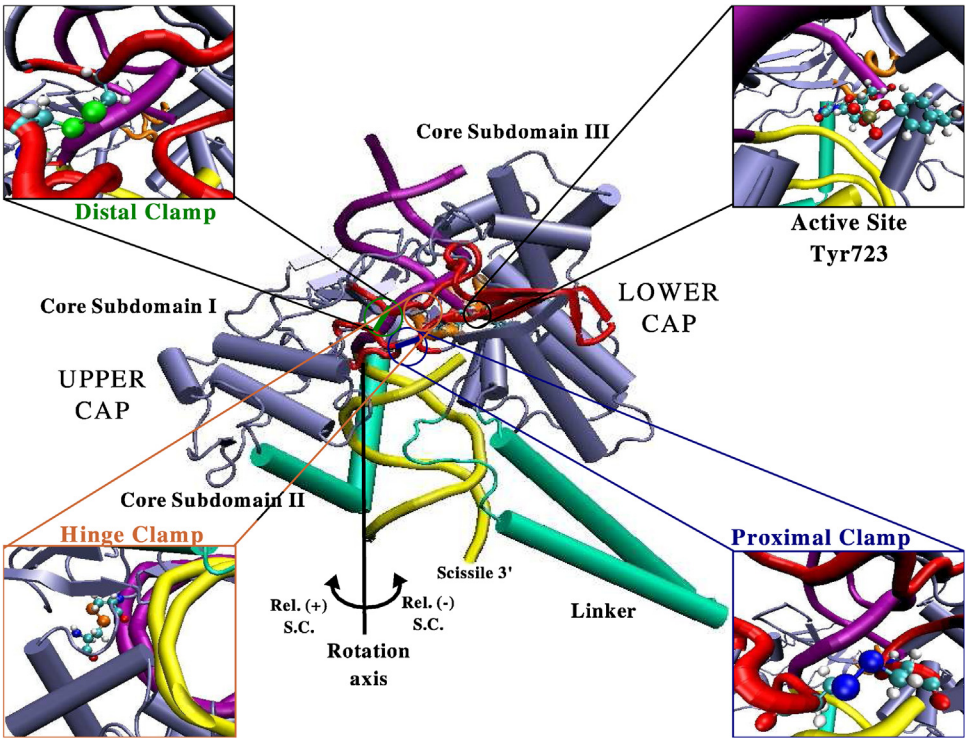

Fig. 1. DNA-human topoisomerase I covalent complex. DNA downstream of the nick is in yellow, upstream DNA in purple, protein is in blue, 'nose-cone' (α5, α6) and the linker helices (α18, α19) are in green, lips region including the 35 residue difference between the distal and proximal clamps are in red, and the hinge region is in orange. Upper and lower caps are also denoted. The rotation axis is shown in black, and directions of rotation for (+) and (−) supercoil relaxation are indicated. **Top left corner**; the disulfide bond in the distally clamped case (shown as a green line in the lips region of the enzyme) is given. **Top right corner**; the phosphodiester bond in the active side is shown. **Bottom left corner**; the disulfide bond in the hinge clamped protein (which is indicated as orange part of the protein) is given. **The bottom right corner**; the disulfide bond in the proximally clamped enzyme (that is shown as a dark blue line on the lips region of the protein) is shown. In the corner figures, the sulfur atoms and the disulfide bonds are shown in green for distally clamped, in orange for the hinge clamped, and in dark blue for the proximally clamped proteins; as they are represented in the same colors in the central figure.

Based on the crystal structures, Champoux and his team have proposed what is now the prevalent model for human topo I activity, the so called 'controlled-rotation' mechanism [10]. In this model, the downstream part of the DNA scissile strand rotates in a manner which is controlled by the surrounding protein, to relax both positive and negative supercoils. However, during strand rotation, whether the protein stays in the closed form or it opens up from the lips region has been a focus of interest, and two seemingly contradictory findings have been published on this issue. In 2003, Champoux's group [11] engineered two cystines into the opposing loops of the lips region (His-367 and Ala-499) that formed a disulfide bond (to which we refer here as the 'distal clamp', in reference to its relative distance from the active site), which is positioned nearby the salt bridge across the opposite lips. They observed that the rate of DNA relaxation in the closed form of the protein is comparable to the unclamped one, and concluded that the relaxation of the DNA occurs in the closed clamp conformation. However, later in the same year, Woo et al. [12] designed a disulfide bond between Gly-365 and Ser-534, also across the two lips, but at a more proximal position to the active site Tyr-723; we shall refer to this disulfide bond as the 'proximal clamp'. Contrary to Champoux's study, they observed that the DNA rotation is inhibited within the locked protein and, moreover, that expression in yeast of the proximally-clamped topo-I complex induced cell death. Because the above studies showed that the two subtle alterations in the flexibility of the enzyme impacted the enzyme's activity differently, it is of fundamental interest to study the extent of protein breathing (or opening) during the strand rotation phase.

In our previous study, we have simulated the 'controlled-rotation' mechanism, starting from the aforementioned crystal structures, and found some un-anticipated mechanistic details for the wild type enzyme [13]. One of them was the observation that the enzyme uses two different mechanisms. To relax positive supercoils, two separate domains (the lips region) of the protein open up by about 10–14 Å, to allow the rotation of DNA because the "cylinder of motion" for DNA duplex rotation around the intact strand has twice the diameter of duplex DNA. In contrast, to relax negative supercoils, because this cylinder of motion contacts a different part of the protein, a continuous loop (which is a hinge for the opposite motion) between the cap and the core subdomain III stretches about 12 Åwhile the lips remain unseparated. In a comprehensive experimental study performed subsequently, Frohlich et al. [14] tested the sensitivity of camptothecin to several mutated enzymes, and observed that some mutated variants are sensitive to camptothecin only during removal of positive supercoils. These results led them to confirm the hypotheses on the difference between positive and negative supercoil relaxation resulting from our theoretical work. At the same time with this experimental confirmation, Chillemi et al. [15] studied the open state of the enzyme by molecular dynamics simulation, and reported large conformational changes during the relaxation mechanism, noting consistence with our findings. In 2008, Xiong et al. [16] studied the mechanism of *Escherichia coli* topoisomerase III, this time a type IA enzyme, and reported that our general findings on type IB enzyme closely mimic their results for type IA topos, where the energy required for opening the central hole is provided by the torque on supercoiled DNA. Most recently, free energy calculations of DNA rotations within the enzyme have been performed [17]; they confirmed different free energy profiles for different sign supercoils, supporting again the hypothesis of distinct relaxation mechanisms

Table 1
The descriptions of the mutations done in the present study.

	Residues mutated to cystines	Initial/final[a] distances (Å)	Represents the work of	Shown in Fig. 1 as
Distally clamped	His367 and Ala499	4.5/5.4	Carey et al. [11]	Green circle, the detail view is given in the upper left corner.
Proximally clamped	Gly365 and Ser534	4.8/6.2	Woo et al. [12]	Blue circle, the detail view is given in the bottom right corner.
Hinge clamped	Leu429 and Lys436	6.6/5.7	See the text.	Orange circle, the detail view is given in the bottom left corner.

[a] Initial distances are measured from the two C_αs in the equilibrated wild type protein. The final distances are measured from the two C_αs in the corresponding equilibrated clamped protein.

for positive vs. negative supercoils, which may find applications in the context of other DNA transactions [18–21] (see also reviews in [22–24]).

As mentioned, our previous simulations were modeling the *wild type* enzyme, and showed that the separations between both the pair Gly365–Ser534 (the residues mutated by Woo et al. [12]) and His367–Ala499 (the residues mutated in the Carey et al. [11] study) increase around 10–14 Å, upon the relaxation of positive supercoils. As we did not observe any distinct behavior in regards to the extent of openings in these two separations in our previous study of the wild type protein, we have carried out and report herein the simulations of the *mutated* clamped enzymes, with exactly the same mutations done by Woo et al. [12] and Carey et al. [11]

Three different mutated protein–DNA systems have been investigated in the present work. First, we have engineered a disulfide bridge between Gly365 and Ser534 by replacing them with cysteines. As this mutation is closer to the active site than the others, this is the 'proximally clamped' enzyme. This mutation is exactly the same as the one experimentally done by Woo et al. [12] Secondly, the 'distally clamped' protein has been prepared, in it the disulfide bridge is patched between His-367 and Ala-499, as done experimentally by Carey et al. [11] In our third system, we have placed a new disulfide linkage between Leu429 and Lys436, to lock the loop region (from Leu429 to Lys436) that we found, for the wild type, to elongate around 12 Å in the process of negative supercoil relaxation while function as a 'hinge' in the relaxation of positive supercoils (see Ref. [13]). This last mutated enzyme is going to be referred to as the 'hinge clamped' protein. As a result of the dynamic simulations on these mutated protein–DNA covalent complexes, we plan to bring an explanation for the aforementioned contradictory experimental observation, and aim to find out more mechanistic details about the supercoil relaxation by human topoisomerase I.

2. Materials and methods

Molecular dynamics simulations were carried out on the CHARMM force field [25] descriptions. Canonical conditions (NVT) were imposed using the Nose–Hoover thermostat [26,27] and taking 2 fs steps by employing the SHAKE algorithm [28]. The non-bonded interactions shifted to zero over 8–12 Å, and the DNA downstream part was biased half-harmonically with an external potential of the form, which is known as Half Quadratic Biased Molecular Dynamics [29]

$$W(r,t) = \frac{\alpha}{2}(\rho - \rho_0)^2, \tag{1}$$

where α is chosen to be 1000 kcal/mole/A^4 (a value adjusted such that a 360° DNA rotation can be feasible within ns time scales). The overall reaction coordinate represented by ρ can be defined as

$$\rho(t) = \frac{1}{N(N-1)} \sum_{i=1}^{N} \sum_{j \neq i}^{N} (r_{ij}(t) - r_{ij}^R)^2 \tag{2}$$

in which $r_{ij}(t) = r_i - r_j$ is the time dependent distance between atoms i and j, and r_{ij}^R is the same distance in the reference set of coordinates. The reference coordinate sets are obtained by applying rigid rotations in 10° increments to the DNA downstream atoms.

A covalent model of the DNA-topoisomerase complex (using crystal structures 1a31.pdb and 1a36.pdb) [9,10] was set up and immersed into a 60 Å-radius sphere of TIP3P [30] water molecules, and charge neutralization was performed by changing 19 waters with sodium ions, where water oxygens had highest electrostatic energies. Three different clamped enzyme-DNA covalent systems were prepared as summarized in Table 1. Cysteines were placed into the positions of interests by changing *only* the side chains of the original residues. In this way, we keep the original position of the backbone atoms unchanged. Then, the disulfide bond was introduced between the two sulfide atoms, and the clamped protein was minimized (within the water box) until a root-mean-square gradient of 10^{-2} kcal/mole, as a result of 1500 steepest descent followed by 1700 steps of adopted basis Newton-Raphson procedure. Then, each system was equilibrated for about 500 ps with the stochastic boundary potential [31] to keep the outmost water molecules. Final separation between the mutated residues in each clamped case is also given in Table 1 (as measured between the two pertinent C_α atoms). Both Intel-Xeon-E5462-64Bit CPUs and Intel-Xeon-X5365-64Bit CPUs are used employing 8 cores in parallel. Each simulation has about 86.000 atoms and 1.8 ns long.

DNA downstream part is rotated around an hypothetical axis that passes through the phosphate of the −1 ADE and phosphate of the +10 ADE on the intact strand, as in the case of previous simulations on the wild type mechanism [13]. The main reason for the choice of the −1 ADE phosphate is two-fold. First, it is exactly opposite to the phosphate on the scissile strand which forms the phosphodiester bond with the protein, and secondly, it sits at the middle of the intact backbone that connects the −1 ADE and +1 ADE. The +10 ADE phosphate is chosen as the second point for the rotation axis, because it sits just below the −1 ADE phosphate in the 3-dimensional structure, making the rotation axis parallel with the helical axis of DNA downstream duplex. We think that such a rotation axis is needed for a proper (with no base-pair opening) rotation as hypothesized by the controlled-rotation' mechanism [10]. Also, our previous predictions [13] on the same rotation axis were well cited by several experimental studies (see the fourth paragraph in Section 1), giving extra confidence in our chose. However, we should also acknowledge the fact that such DNA rotations bias the simulation results. This is mainly because the rotating DNA segment is as if a stiff rod rotation (although not exactly due to harmonic nature of the external potential) with limited freedom for DNA internal conformational changes. This may force the protein to undergo more conformational changes then it would need to for a flexible DNA molecule. The reader should keep this point in mind when evaluating our results.

Another important point that needs to be mentioned is about the long-range electrostatics. We have employed stochastic boundary conditions, immersing the system into a spherical water box, rather than employing periodic boundary conditions. Therefore, Particle Mesh Ewald (PME) is not suitable for long-range electrostatics. The non-bonded interactions are shifted to zero over 8–12 Å, ignoring any possible effects of long range electrostatics. In principal, we would choose a much longer range for non-bonded

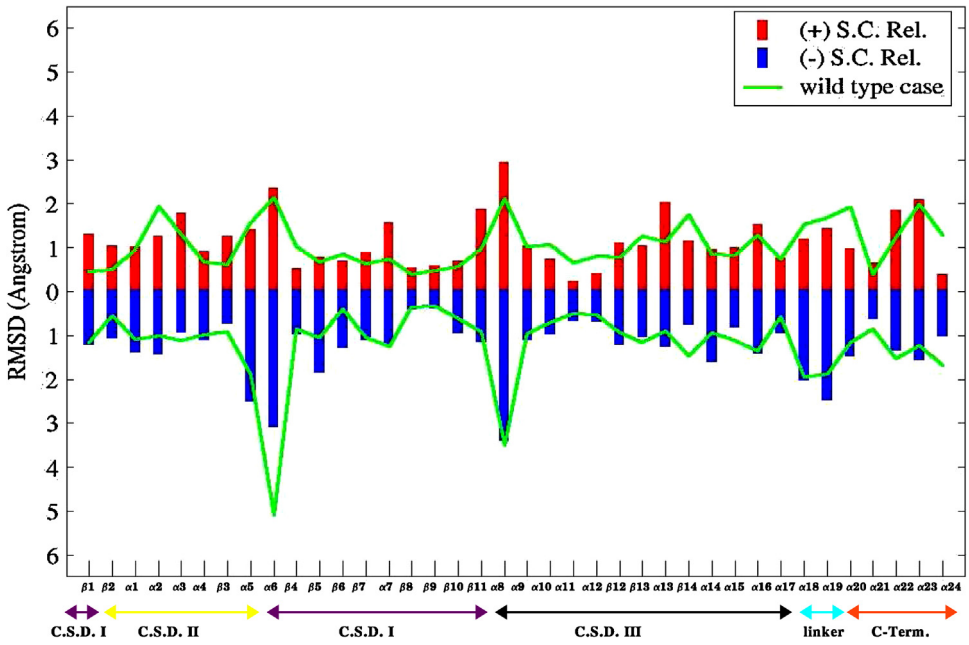

Fig. 2. The RMSD between the initial and the final geometries of the each secondary structure when the distal clamp is engineered. The green curves shows the allowed values in the wild type case. The red bars shows the deformations upon the rotation of the downstream DNA that relaxes (+) supercoils. Similarly, the blue bars shows the RMSD values upon (−) supercoil relaxations. (For interpretation of the references to color in this figure legend, the reader is referred to the web version of the article.)

interactions, making the simulations much more accurate for such a highly charged nucleic acid system. Here, we have used exactly the same cut off distances that we used before on wild type system. Unavoidably, this also imposes some limitations on the dynamics, and on the accuracy of final results presented here.

All of the other details of the equilibration and production level molecular dynamics calculations are exactly the same as those employed for the wild type case, and we refer the reader to Ref. [13] for more theoretical details.

3. Results and discussion

As we biased the DNA rotation with an external potential, and therefore bring the full 360° rotation of the DNA downstream in all clamped-enzyme simulations, the way to get information about whether these clamped proteins can in fact let DNA rotate or not is to compare the clamped-enzyme simulations with the wild-type case, and meanwhile look for any *distinct* behavior in the clamped cases. Therefore, both structural and energetic comparisons between the clamped protein systems and the wild type protein system are going to be considered. In structural comparison, the root mean square deviations (RMSD) of the final geometries (at the end of DNA rotations) of each secondary structure are calculated by superimposing the final geometry on top of the initial geometry. These RMSD values show the amount of deformations in the secondary structures of each clamped protein system when the DNA is rotated.

The calculated RMSD values are plotted in Fig. 2 for the distally clamped case, in Fig. 3 for the proximally clamped case, and in Fig. 4 for the hinge clamped case. As seen in Fig. 2, all deformations in the secondary structures are very similar to those of the wild type case when the substrate DNA is positively supercoiled. In the case of relaxation of negative DNA supercoils (blue color in Fig. 2), the situation is the same except for a relatively smaller deformation in the α6 subunit compared to the wild type case. Other than this, there are some minor *extra* deformations (compared to the wild type case, see the Fig. 2), which are 0.83 Å for β1, 0.78 Å for α7, 0.86 Å for β11, 0.77 Å for α8, and 0.86 Å for α13 when the substrate DNA is positively supercoiled, and very similar values (around 0.7 Å) for a couple of subunits (α5, β5, α14, and α19) in the relaxation of negative supercoils. These small values that are within ±1 Åcan be regarded as within the range of thermal noise thus negligible in our nanosecond time-scale biased simulations. Therefore, when the protein is locked from the distal points (as was done by Carey et al. [11]), the deformations in the secondary structures of the protein during DNA rotations are well within the values of the wild type protein.

However, when we plot the deformations (RMSDs) for the proximally clamped enzyme, in exactly the same way that we did for the distally locked one, we have, interestingly, observed a very large deformation in α5 (in core subdomain II), that was not observed in the distally clamped protein. As seen in Fig. 3, the helix α5 collapses almost entirely, with an RMSD of 5.74 Å (while it is only 1.56 Å in the wild type case and about 1.35 Å for the distally clamped one) at the end of the rotation of DNA for the removals of positive supercoils. The melting of helix α5 is also shown in Fig. 5 where its initial and final shapes after the rotations under three different cases (wild, distally clamped, and proximally clamped) are depicted. As it is clear in the figure, α5 preserves its internal structure in both wild type and distally clamped cases, whereas it unfolds in the case of proximally clamped enzyme. The large deformation in α5 is tested with two other simulations, one with a shorter timescale of 1.08 ns and the other with a longer timescale of 3.6 ns. As seen in Fig. 5, large RMSD values of 6.50 Å and 6.82 Å are obtained correspondingly. Interestingly, in relaxation of negative supercoils, α5 behaves almost identical to the case of wild type protein, both in the distally and proximally clamped systems.

The relatively lower RMSD values for α6 in the clamped cases of negative supercoil relaxations might be unexpected, although the differences are only around 2 Å. This is the largest deviation between wild type and clamped protein systems in the relaxation of negative supercoils (all other deviations are well within 1 Å). The main reason for this observation might be the fact that helix α6 is on the other side of the lips region where clamps are introduced. Therefore, clamping the protein on the lips side gives α6 more freedom on the other side during DNA rotations, causing less

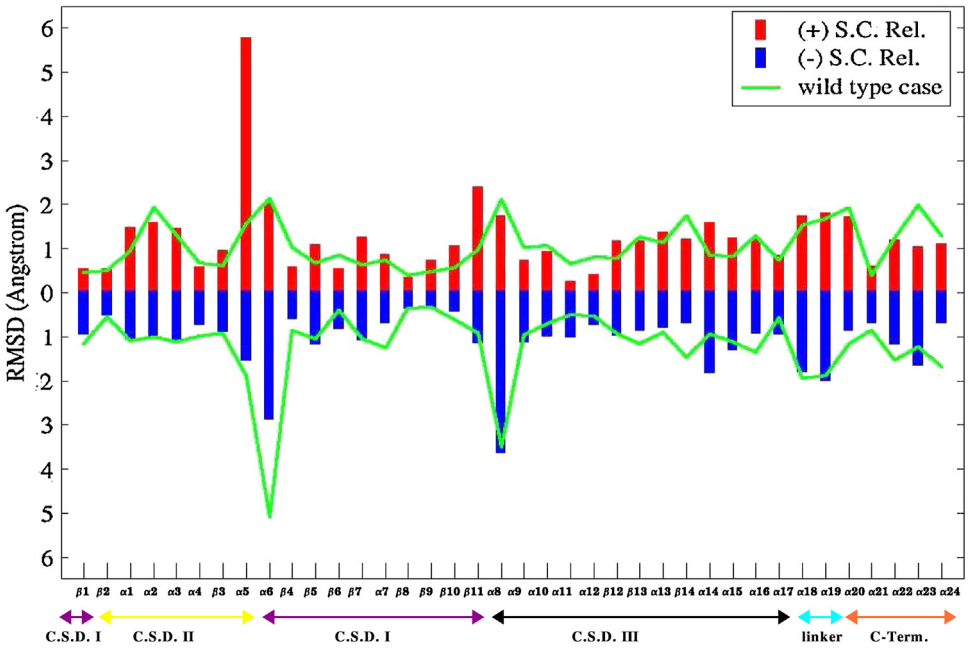

Fig. 3. The same RMSD picture described in Fig. 2, but for the proximally clamped enzyme.

deformations. That is also why $\alpha 5$ deforms a lot in the clamped cases, because it is on the side of the lips region (just at the top of the lips), and clamping protein on that side restricts its rigid body motion, forcing it to deform a lot.

To elaborate this interesting finding, we have analyzed the applied potential energy in relaxations of positive supercoils as a function of the reaction coordinate. Fig. 6 shows the results for DNA rotations between 40 degrees and 80 degrees, as the deformation in $\alpha 5$ starts in this part of the full rotation. In the figure, each plot corresponds to a 10 degree rotation. We see that the proximally clamped system moves further than both wild and distally clamped proteins, with large applied external potentials of around 2–3 kcal/mole. However, as seen in the figure, the applied potentials to bring the DNA rotations within the wild and distally clamped protein systems are very similar in magnitudes, only around 0.5–1 kcal/mole. This means that the proximally clamped protein is nonphysically forced to be able to allow the DNA rotations in our biased molecular dynamic simulations. This explains why the protein deforms when it is clamped proximally, while it stays undeformed when it is clamped distally.

In regards to energetic comparisons, the interaction energy (sum of van der Waals and electrostatic interactions) between protein and the DNA is focused upon next, for both clamped proteins and wild type protein systems. The interaction energies between each secondary structures of the protein and DNA are calculated, both at the beginning and at the end of rotations. Although interaction energies are calculated and reported for all secondary structures, the main attention here will be given to 'nose-cone'

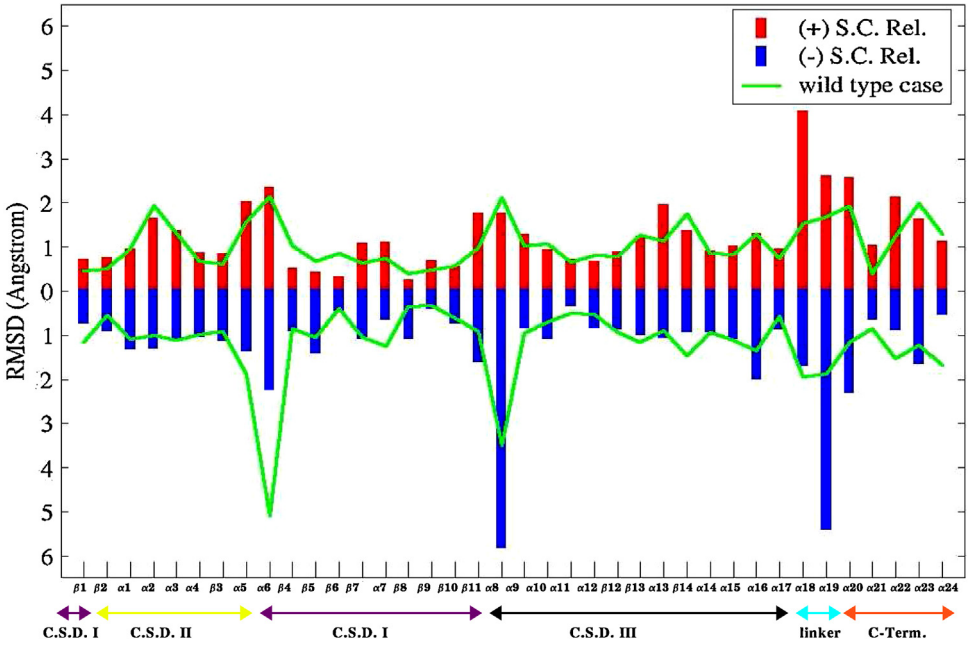

Fig. 4. The same RMSD picture described in Fig. 2, but for the hinge clamped enzyme.

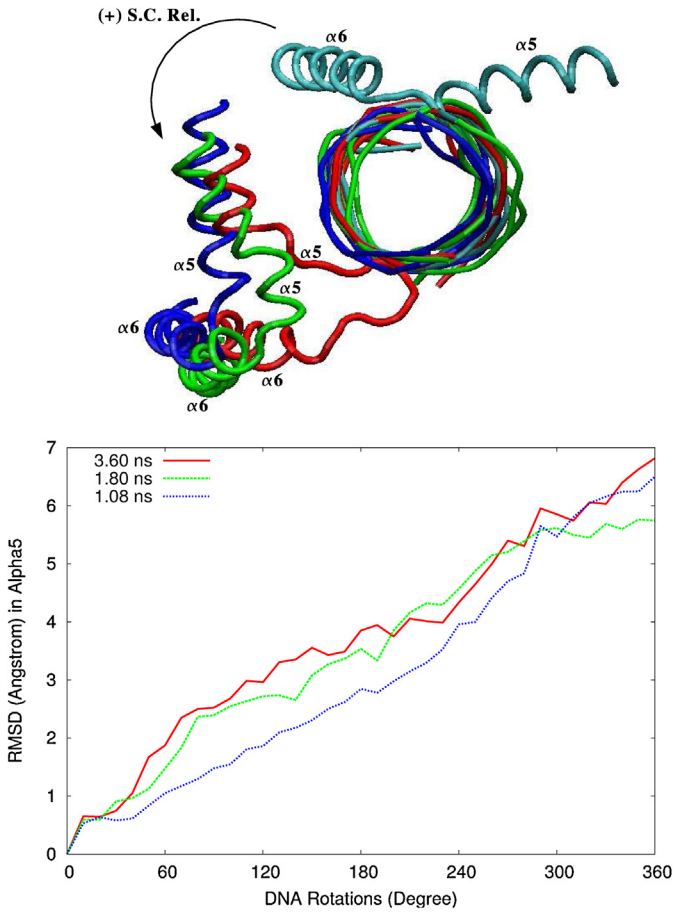

Fig. 5. Top: The initial and the final [after the rotation that relaxes (+) turns] shapes of the 'nose-cone' helices. The initial structure is in cyan, the final structure in the wild type protein is in green, that of distally clamped protein is in blue, and that of proximally clamped one is in red. Initial and the final structures of DNA are also shown in the same coloring scheme. Note the *distinct* deformation of the helix in the case of proximally clamped protein, shown in red. **Bottom**: The RMSD deformations in α5 in relaxation of (+) DNA supercoils within the proximally clamped enzyme. The same simulations with three different time-scales. (For interpretation of the references to color in this figure legend, the reader is referred to the web version of the article.)

helices (α5 and α6), the linker (α18 and α19), and the hinge helix (α8). This is because these are the regions of the enzyme that have been thought to be important in controlling DNA rotations [9,10,32,33], and melting is seen here in α5 unit of the proximally clamped protein. It should be emphasized that these energies correspond just two points (initial and final) along the reaction coordinate. Normally, free energy profiles must be determined to get the definitive energetics. We plan to get such free energy profiles in an another study, although it seems to be quite computationally intensive. In this line, we have analyzed all sorts of interaction energies including protein–DNA, protein–solvent, protein internal, DNA internal, protein domain–domain interactions, etc. However, we could not deduce a meaningful qualitative picture based on these energetics. This is because, the scale of these energetics are on the order of thousand kcal/mole (corresponding to thousands of atoms), and changes are quite large as we do a biased MD with external potential.

The interaction energy of each α and β subunits of the protein with the DNA atoms are given in Fig. 7 for the removal of positive supercoils, and in Fig. 8 for the removal negative supercoils. When we look at the interaction energies for the relaxations of positive supercoils (Fig. 7), and compare the distally and proximally clamped protein systems with the wild type case, we see the differences in α5, α16, and α23. The helix α5 has a total interaction energy of 177 kcal/mole with the DNA at the beginning of the rotations. It loses much of this energy in both wild and distally clamped enzymes, decreasing to 27 kcal/mole in the wild type case and 47 kcal/mole in the distally clamped case. However, in the proximally clamped protein, this interaction energy reduces to only 142 kcal/mole. The reason for this is the collapse of the helix around DNA within the proximally clamped protein. As seen in Fig. 5, α5 gets away from the DNA more or less the same amount of distances in both wild and distally clamped cases, while it melts and gets bounded to DNA at the end of the rotation within the proximally clamped protein. Therefore, total collapse of this helix in the proximally clamped system would mean that such clamping will totally make the enzyme nonfunctional for *positive* DNA supercoil relaxation. In our previous study on the wild type mechanism [13], we have found that helix α5 (as being the right nose-cone helix) play important roles in relaxations of *positive* DNA supercoils, which is in agreement with the current finding.

The helix α23, which is in the C-terminal domain containing the active site, has also the same behavior in wild and distally clamped cases, while it shows different energetics in the proximally clamped protein. It has an initial interaction energy of 190 kcal/mole that decreases to 179 kcal/mole at the end of DNA rotation within the wild type enzyme. The same energy is 221 kcal/mole for the distally clamped one, that is 42 kcal/mole larger than the wild type case. However, in the proximally clamped protein it drops quite significantly, to a value of only 95 kcal/mole, as seen in Fig. 7. Therefore, both structural and energetic analyses suggest that relaxation of a *positively* supercoiled DNA should be inhibited if the protein is clamped proximally, while rotations within the distally clamped protein are similar to the wild type enzyme.

When we look at the interaction energies for the relaxation of *negatively* supercoiled DNA, we see that both type clampings (distal and proximal) exhibit almost similar signatures with the wild type protein. If we look at the corresponding blue bars in Fig. 8, the only noticeable difference is seen to be for the unit β11. At the initial state, the unit does not interact with DNA much, but at the end of the rotations in both wild type and distally clamped proteins, it gets close to DNA and gains appreciable interaction energies (around 135 kcal/mole for wild type and 170 kcal/mole for the distally clamped case). However, in the case of proximally clamped protein it is ended up again with a very small interaction of around 20 kcal/mole. Other than this, in the proximally clamped protein, helices α5, α6, and α8 ended up with interaction energies a little smaller than those of the wild and distally clamped cases. Considering the aforementioned fact that (in relaxation of *negatively* supercoiled DNA) the deformations for both distally and proximally clamped systems are well within the deformations of the wild type protein (see the blue bars in Figs. 2 and 3), we can say that the relaxation of a *negatively* supercoiled DNA should not be hindered much both in the distally clamped protein and in the proximally clamped protein.

At this point, the question that needs to be answered is the following; what kind of DNA supercoils (positive or negative) were used in the studies of Carey et al. [11] and Woo et al. [12], as they draw opposite conclusions. In the study of Woo et al. [12], authors clearly state that they used EtdBr to produce positive supercoils and no change in the linking number was observed when the protein is locked (on page 13771 of their paper). This is nicely in accordance with our aforementioned theoretical predictions that the relaxation of positively supercoiled DNA should be hindered within the proximally locked enzyme. The type of supercoil used by the Carey et al. [11] is not explicitly mentioned in their paper, but can be inferred. They test whether or not the clamped protein is capable of relaxing supercoils produced by the temperature shifts. They increase the temperature of the locked enzyme-DNA system from

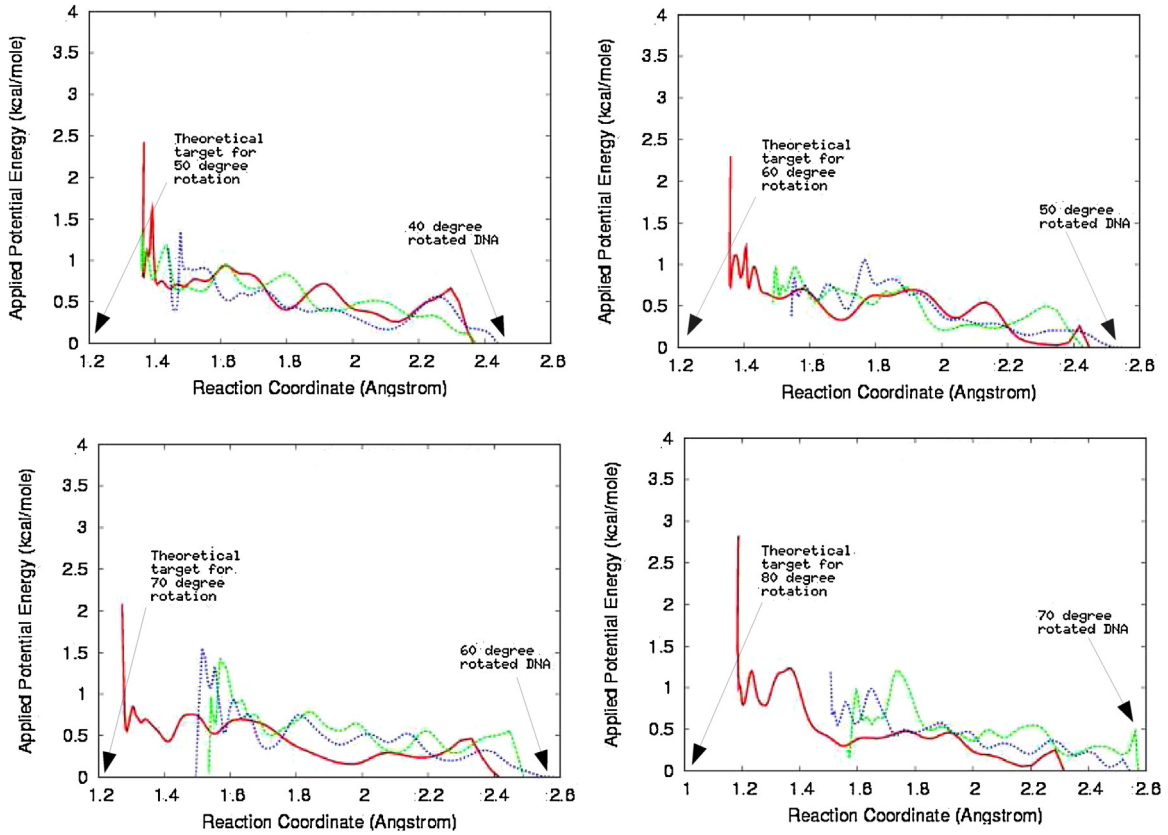

Fig. 6. Amount of time dependent potential energy applied to get the DNA rotations within proximally clamped (red lines), distally clamped (green lines), and wild type proteins (blue lines). Only rotations from 40 degree to 80 degree are shown, as the unphysical deformation in the proximally clamped protein starts in this range. The reaction coordinate (x-axis), is the average distance to the target, that is $\sqrt{\rho(t)}$ where $\rho(t)$ is given in Eq. 2. (For interpretation of the references to color in this figure legend, the reader is referred to the web version of the article.)

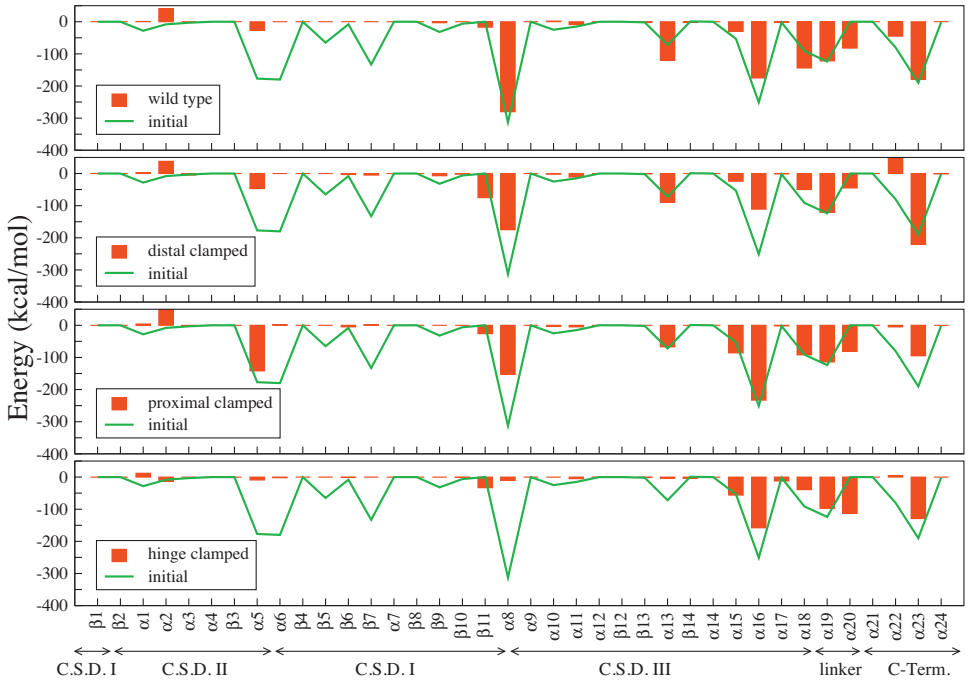

Fig. 7. Change in the interaction energy of the each secondary structure with DNA, as the DNA rotates to relax positive supercoils. The green line shows the initial interaction energies with DNA. The four graphs corresponds, from top to bottom, to wild type protein, distally clamped protein, proximally clamped protein, and hinge clamped protein. (For interpretation of the references to color in this figure legend, the reader is referred to the web version of the article.)

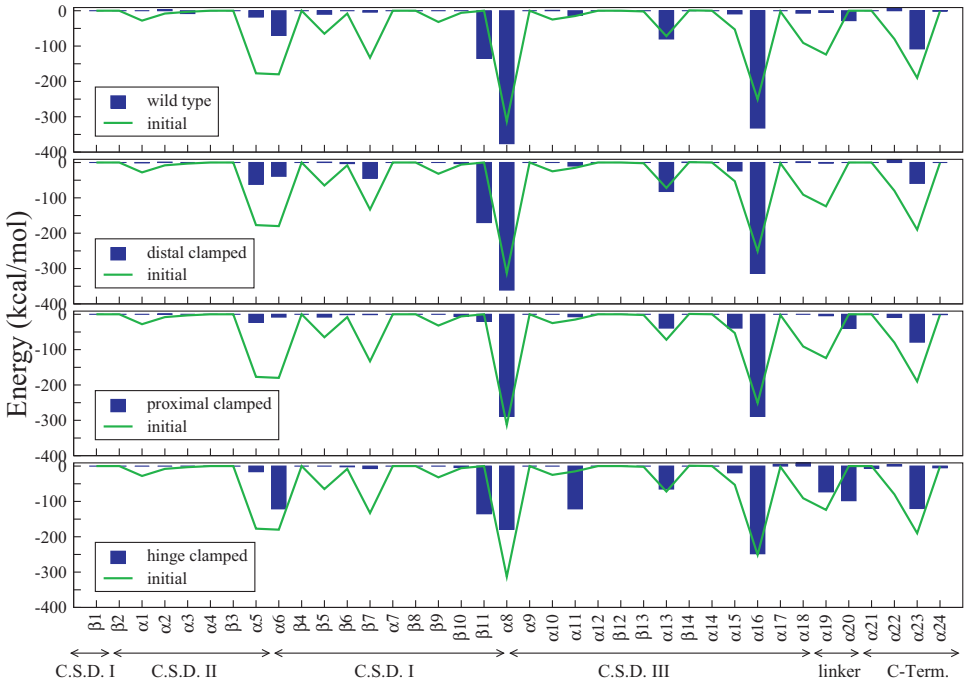

Fig. 8. The same graph as the Fig. 7, except for the relaxation of (−) supercoils.

4 °C to 23 °C, and they analyzed the mobilities of topoisomers by agarose gel electrophoresis. They reported that the locked enzyme is *able* to relax supercoils that occurred due the temperature shifts (they also test for 37 °C, and observe the same). The temperature dependency of DNA supercoils is well known: less winding (more negative supercoils) as the temperature is increased [7,34,35] (an average of −0.012 degrees/°C for the helix rotation angle, and a value of -3.5×10^{-4} for $1/\mathrm{Lk_0}^*(\mathrm{dLk_0}/\mathrm{d}T)$ was reported by Wang C. and co-workers [34]. For a closed plasmid DNA, as the linking number (Lk) is a topological invariant, and thus does not change, $\mathrm{Lk}-\mathrm{Lk_0}$ increases producing less negative supercoils (i.e., relatively positive supercoils). Therefore, what Carey et al. [11] observe are extra positive supercoils relaxed by the locked-enzyme (see also discussion in Froclich et al. [14]). This result is also in agreement with our theoretical observations here that the relaxation of positive supercoils should not be hindered within the distally clamped enzymes. In fact, the distally clamped enzyme behaves very much like the wild type enzyme for both positive and negative supercoils, and therefore the sign of supercoil used in Carey et al. [11] study does not matter too much for the main discussion here. In brief, in light of our theoretical simulations, we are able to conclude that both experiments by Carey et al. [11] and Woo et al. [12] are *perfectly* fine, and what they observed are just correct pictures. The seemingly controversial conclusions that they draw is just due to the fact that position of disulfide bridge in the lips region of the protein is crucial, as the breath of the enzyme for DNA rotations is impeded if the bridging happens to be in the proximal side, while distal bridging does not hinder the DNA rotations. To summarize this discussion, we can conclude the following:

Our current theoretical results suggest that: (i) the locked protein mutant of Carey et al. [11] should be able to relax both positive and negative supercoils; (ii) the locked protein mutant of Woo et al. [12] is *not* able to relax positive supercoils, while it is able to relax negative supercoils; and (iii) small changes in the position of disulfide bridge give rise to significant changes in the enzyme behavior towards DNA rotations.

It is also important to note that the protein used in the study of Carey et al. is an N-terminally truncated protein, while Woo et al. used a full length protein. The structurally undefined N-terminal domain is known to be important in protein–protein interactions, and in the nuclear localization of the enzyme [8,36–39], as it is found to be dispensable [40] for the enzyme activity *in vitro*. In fact, in 2008, Palle et al. [41] engineered both distal and proximal disulfide bridges and tested for the activity of both full length and N-terminally truncated enzyme. They observed that formation of disulfide bonding in the distally clamped full-length enzyme occurs more readily in the absence of DNA than with proximally clamped enzyme. They attributed this difference to a severe defects in binding of the distally clamped protein to the DNA, and conclude that the disulfide bond formation happens to be prior to DNA binding *in vivo* (see page 27774 of their paper). They observed that the N-terminal domain is needed for the stability and full activity *in vivo*, while no data suggests that the DNA relaxation observed by Carey et al. is due to the absence of the N-terminal domain. In fact, they argued that the possibility exists that subtle alterations in enzyme architecture might profoundly affect enzyme activity [12,41], which is exactly what our simulations show.

The hinge clamped enzyme

In our previous study on the wild type mechanism, we have observed that the 'hinge' region (see Section 1 for the definition) stretches around 12 Å in the relaxation of negative supercoils while it stays unchanged during the opposite DNA rotation [13]. Therefore, we would expect large deformations in the enzyme when we clamp the hinge and force DNA rotations to relax negative supercoils. We plot the RMSD deviations in each secondary structure of the hinge-clamped protein in Fig. 4, and the interaction energy patterns are given in Fig. 7 and in Fig. 8 for the relaxation of positive and negative supercoils respectively. As expected, in the relaxation of negative supercoils, the locked enzyme shows very large deformations in $\alpha 8$ and $\alpha 19$, as the RMSD value of 5.9 Å and 5.4 Å are obtained respectively for $\alpha 8$ and $\alpha 19$. Therefore, in the relaxation of negative supercoils, it is clear that the RMSD signature of the wild type enzyme is quite changed once the enzyme is locked from the hinge region. In relaxation of positive supercoils, the deformation in the locked enzyme occurs to a much lesser extent, as expected. In this case, we have observed very similar RMSD values for wild

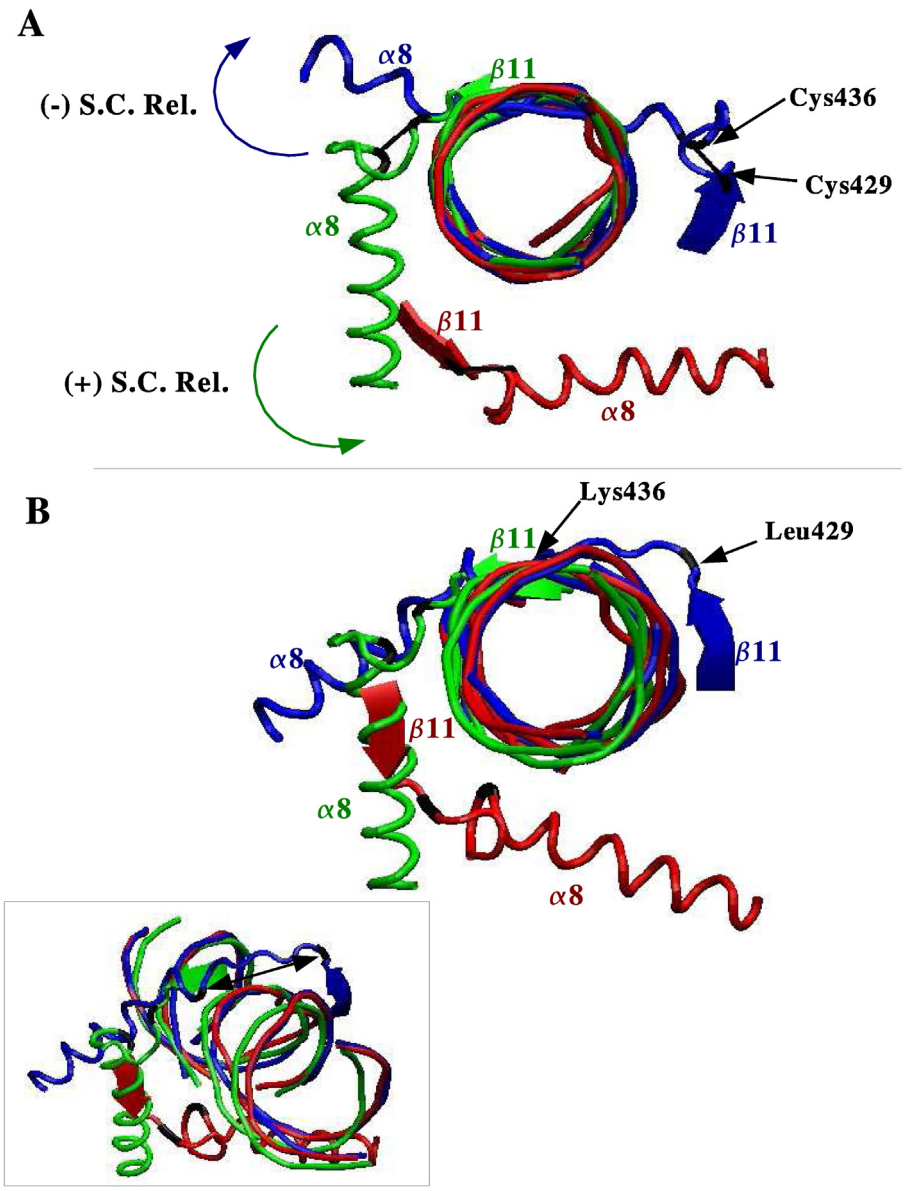

Fig. 9. The initial and the final shapes of the helix α8 after both rotations. The green ones represents its initial structures, the blue ones are the shapes at the end of (−) supercoil relaxation, and the red ones are those obtained at the end of (+) supercoil relaxation. **A** When the protein is locked from the hinge region, **B** in the case of wild type protein. The wild type case is also given in the bottom left corner from a different perspective, where the stretch in the hinge (from Leu429 to Lys436) is clear upon the relaxation of (−) turns. Note the large deformation upon the relaxation of (−) supercoils, when the enzyme is locked (shown in part A). (For interpretation of the references to color in this figure legend, the reader is referred to the web version of the article.)

type and locked enzyme cases, except for α18 in the linker region, which has extra deformations in the locked protein system. This might be due to the correlated functions of hinge with the linker domain, as previously suggested by Chillemi et al. [42]

To analyze the hinge region in more detail, we have pictured the shape of α8, β11, and the loop in between the two, in Fig. 9 for both rotations. In the top part of the figure, the hinge clamped system is presented with a black line showing the disulfide bridge. The same picture for the wild type case is also given in the bottom part of the figure. As seen in the figure, the helix α8 (the largest secondary structure in size, and has the largest initial interaction energy with DNA) rearranges substantially upon the rotation that relaxes negative supercoils, while it preserves its shape very well upon the relaxation of positive supercoils. The reason for this is clear; in the wild type mechanism, the clamped distance stretches around 12 Å to accommodate DNA rotation [13], as shown in the bottom part of the figure. When the loop that is stretched is clamped, DNA rotation forces α8 to unfold nonphysically, so that it can accommodate the biased rotation. However, in the case of positive supercoils, both α8 and the hinge region nicely preserve their internal structures in both wild and clamped cases, as seen in the figure. It may also worth noting that α8 loses its interaction energy with DNA in relaxation of positive supercoils, when the enzyme is clamped. This is a result of its rigid body movement away from DNA, as its RMSD is almost identical to that of wild type case. Therefore, although we cannot come to any definitive conclusion on the possibility of the relaxation of positive DNA supercoils within the hinge clamped enzyme, it is very probable that the rotation profile will get affected once the enzyme is clamped in the hinge region, as suggested by the lost of interaction energy with DNA.

We have also observed that the linker (helices α18 and α19) deform after the DNA rotations within the hinge locked enzyme. This is interesting, because for the other two clamped systems (distally and proximally clamped cases), we have observed that the

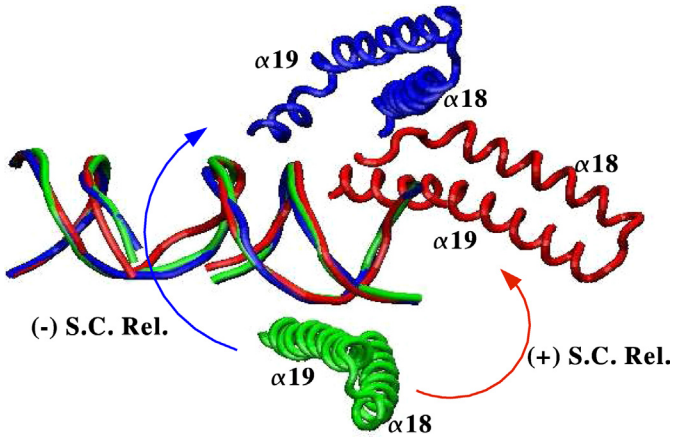

Fig. 10. The initial and final geometries of linker helices, before and after DNA rotations within hinge clamped enzyme. The initial structure is in green, that of after positive relaxation is in red, and that of after negative relaxation is in blue. (For interpretation of the references to color in this figure legend, the reader is referred to the web version of the article.)

linker helices have very similar RMSD values with those of the wild type case (see Figs. 2 and 3). It is also interesting that, in the relaxation of positive supercoils, helix α18 of the linker deforms (with an RMSD of 4 Å) while the helix α19 stays similar to the wild type case. In the relaxation of negative supercoils, the situation is exactly vice versa; α19 deforms (with an RMSD of 5.4) while α18 stay similar to the wild type case. To get deeper insight, we have pictured the shapes of linker helices before and after DNA rotations. As given in Fig. 10, deformation is seen to be at the beginning part of helix α18 for positive supercoil relaxations (red color in the figure), and somewhere between the beginning and middle part of the helix α19 for negative supercoil relaxations. The observed deformations in the linker region in the hinge clamped enzyme suggest a correlated functionality of the linker with the residues in the hinge region. In fact, Chillemi et al. [42] carried out dynamic cross correlation (DCC) map of the protein, and observed strong anti-correlated motions (correlated motions in the opposite directions) between the linker residues and α8. More recently, the same group examined the role of linker domain in the catalytic activity, and found the existence of long-range communications between linker and active site. Together with these findings, our observations of large deformations in linker domain in the hinge-clamped enzyme show that the linker plays an important role during DNA rotations, as suggested previously for the wild type enzyme [13].

4. Conclusion

The current simulations on the three different human topoisomerase I-DNA covalent complex shed light on the seemingly contradictory results obtained by Carey et al. [11] and Woo et al. [12] Our simulations show that a distally clamped enzyme (as that of Carey et al. [11]) can relax both positive and negative supercoils, while a proximally clamped enzyme (the one in Woo et al. [12]) can relax *only* negative supercoils. With this observation in hand, when we look at the sign of DNA supercoils that the two group of researchers used in their experiments, we see that positive supercoils are used in both study. Therefore, although Carey et al. do not see any problem in relaxation, the relaxation of *positive* DNA supercoils formed in the study of Woo et al. [12] hindered mainly by the nose-cone helix α5 (the right nose-cone helix, as defined by Champoux and coworkers [9,10]). Our results here show that the small changes in the location of disulfide bridge brings significant changes in the behavior of the enzyme, and this is exactly the reason for the opposite conclusions that the two group report. Additionally, current simulations suggest that clamping the enzyme in the hinge region should result in the inhibition of negative DNA supercoils, but not the positive ones. Also, we have seen deformations in the linker helices when the enzyme is locked from the hinge region, and moreover, these deformations are dependent on the sign of supercoils that the DNA has. This is in support of our previous finding that the relaxation mechanisms for negative and positive DNA supercoils are different [13], and produces different conformational changes in the enzyme. The results herein may be used to design molecular motors from mutant enzymes that relax one sign of the supercoils preferentially and suggest novel clamps that can be engineered in the hinge region.

Acknowledgments

This work is supported by The Scientific and Technological Research Council of Turkey (TUBITAK) under the grant 107T209. We also thank Professor James J. Champoux from the University of Washington-Seattle for his valuable informations that he share with us.

Appendix A. Supplementary data

Supplementary data associated with this article can be found, in the online version, at http://dx.doi.org/10.1016/j.jmgm.2013.07.003.

References

[1] S.J. Brill, S. Dinardo, K. Voelkelmeiman, R. Sternglanz, Need for DNA topoisomerase activity as a swivel for DNA-replication for transcription of ribosomal-RNA, Nature 326 (1987) 414–416.
[2] Y.P. Tsao, H.Y. Wu, L.F. Liu, Transcription-driven supercoiling of DNA – direct biochemical-evidence from in vitro studies, Cell 56 (1989) 111–118.
[3] C. Holm, T. Stearns, D. Botstein, DNA topoisomerase-II must act at mitosis to prevent nondisjunction and chromosome breakage, Molecular and Cellular Biology 9 (1989) 159–168.
[4] D. Rose, W. Thomas, C. Holm, Segregation of recombined chromosomes in meiosis-I requires DNA topoisomerase-II, Cell 60 (1990) 1009–1017.
[5] V. Bohr, DNA repair and transcriptional activity in genes, Journal of Cell Science 90 (1988) 175–178.
[6] L. Postow, N.J. Crisona, B.J. Peter, C.D. Hardy, N.R. Cozzarelli, Topological challenges to DNA replication: conformations at the fork, Proceedings of the National Academy of Sciences of the United States of America 98 (2001) 8219–8226.
[7] J.C. Wang, DNA topoisomerases, Annual Review of Biochemistry 65 (1996) 635–692.
[8] J.J. Champoux, DNA topoisomerases: structure, function, and mechanism, Annual Review of Biochemistry 70 (2001) 369–413.
[9] M.R. Redinbo, L. Stewart, P. Kuhn, J.J. Champoux, W.G.J. Hol, Crystal structures of human topoisomerase I in covalent and noncovalent complexes with DNA, Science 279 (1998) 1504–1513.
[10] L. Stewart, M.R. Redinbo, X.Y. Qiu, W.G.J. Hol, J.J. Champoux, A model for the mechanism of human topoisomerase I, Science 279 (1998) 1534–1541.
[11] J.F. Carey, S.J. Schultz, L. Sisson, T.G. Fazzio, J.J. Champoux, DNA relaxation by human topoisomerase I occurs in the closed clamp conformation of the protein, Proceedings of the National Academy of Sciences of the United States of America 100 (2003) 5640–5645.
[12] M.H. Woo, C. Losasso, H. Guo, L. Pattarello, P. Benedetti, M.A. Bjornsti, Locking the DNA topoisomerase I protein clamp inhibits DNA rotation and induces cell lethality, Proceedings of the National Academy of Sciences of the United States of America 100 (2003) 13767–13772.
[13] L. Sari, I. Andricioaei, Rotation of DNA around intact strand in human topoisomerase I implies distinct mechanisms for positive and negative supercoil relaxation, Nucleic Acids Research 33 (20) (2005) 6621–6634, http://dx.doi.org/10.1093/nar/gki935, ISSN 0305-1048.
[14] R.F. Frohlich, C. Veigaard, F.F. Andersen, A.K. McClendon, A.C. Gentry, A.H. Andersen, N. Osheroff, T. Stevnsner, B.R. Knudsen, Tryptophane-205 of human topoisomerase I is essential for camptothecin inhibition of negative but not positive supercoil removal, Nucleic Acids Research 35 (18) (2007) 6170–6180, http://dx.doi.org/10.1093/nar/gkm669, ISSN 0305-1048.
[15] G. Chillemi, A. Bruselles, P. Fiorani, S. Bueno, A. Desideri, The open state of human topoisomerase I as probed by molecular dynamics simulation, Nucleic Acids Research 35 (9) (2007) 3032–3038, http://dx.doi.org/10.1093/nar/gkm199, ISSN 0305-1048.
[16] B. Xiong, D.L. Burk, J. Shen, X. Luo, H. Liu, J. Shen, A.M. Berghuis, The type IA topoisomerase catalytic cycle: a normal mode analysis and molecular

dynamics simulation, Proteins: Structure, Function, and Bioinformatics 71 (4) (2008) 1984–1994, http://dx.doi.org/10.1002/prot.21876, ISSN 0887-3585.
[17] J. Wereszczynski, I. Andricioaei, Free energy calculations reveal rotating-ratchet mechanism for DNA supercoil relaxation by topoisomerase IB and its inhibition, Biophysical Journal 99 (3) (2010) 869–878, http://dx.doi.org/10.1016/j.bpj.2010.04.077, ISSN 0006-3495.
[18] P. Fiorani, C. Tesauro, G. Mancini, G. Chillemi, I. D'Annessa, G. Graziani, L. Tentori, A. Muzi, A. Desideri, Evidence of the crucial role of the linker domain on the catalytic activity of human topoisomerase I by experimental and simulative characterization of the Lys681Ala mutant, Nucleic Acids Research 37 (20) (2009) 6849–6858, http://dx.doi.org/10.1093/nar/gkp669, ISSN 0305-1048.
[19] O. Szklarczyk, K. Staron, M. Cieplak, Native state dynamics and mechanical properties of human topoisomerase I within a structure-based coarse-grained model, Proteins: Structure, Function, and Bioinformatics 77 (2) (2009) 420–431, http://dx.doi.org/10.1002/prot.22450, ISSN 0887-3585.
[20] J. Bozzo, C. Dulsat, Therapeutic targets for melanoma, Drugs of the Future 33 (7) (2008) 615–631, http://dx.doi.org/10.1358/dof.2008.033.07.1236495, ISSN 0377-8282.
[21] G.S. Laco, Y. Pommier, Role of a tryptophan anchor in human topoisomerase I structure, function and inhibition, Biochemical Journal 411 (Part 3) (2008) 523–530, http://dx.doi.org/10.1042/BJ20071436, 0264-6021.
[22] A.J. Schoeffler, J.M. Berger, DNA topoisomerases: harnessing and constraining energy to govern chromosome topology, Quarterly Reviews of Biophysics 41 (1) (2008) 41–101, http://dx.doi.org/10.1017/S003358350800468X, ISSN 0033-5835.
[23] M. Orozco, A. Noy, A. Perez, Recent advances in the study of nucleic acid flexibility by molecular dynamics, Current Opinion in Structural Biology 18 (2) (2008) 185–193, http://dx.doi.org/10.1016/j.sbi.2008.01.005, ISSN 0959-440X.
[24] A.D. MacKerell Jr., L. Nilsson, Molecular dynamics simulations of nucleic acid–protein complexes, Current Opinion in Structural Biology 18 (2) (2008) 194–199, http://dx.doi.org/10.1016/j.sbi.2007.12.012, 0959-440X.
[25] B.R. Brooks, R.E. Bruccoleri, B.D. Olafson, D.J. States, S. Swaminathan, M. Karplus, CHARMM: a program for macromolecular energy, minimization, and dynamics, Journal of Computational Chemistry 4 (1983) 187–217.
[26] S. Nosé, A unified formulation of the constant temperature molecular-dynamics methods, Journal of Chemical Physics 81 (1984) 511–519.
[27] W.G. Hoover, Canonical dynamics—equilibrium phase-space distributions, Physical Review A 31 (1985) 1695–1697.
[28] J. Ryckaert, G. Ciccotti, H. Berendsen, Numerical integration of the Cartesian equations of motion of a system with constraints: molecular dynamics of n-alkanes, Journal of Computational Physics 23 (1977) 327–341.
[29] E. Paci, M. Karplus, Forced unfolding of fibronectin type 3 modules: an analysis by biased molecular dynamics simulations, Journal of Molecular Biology 288 (1999) 441–459.
[30] W.L. Jorgensen, J. Chandrasekhar, J.D. Madura, R.W. Impey, M.L. Klein, Comparison of simple potential functions for simulating liquid water, Journal of Chemical Physics 79 (1983) 926–935.
[31] C.L. Brooks, A. Brunger, M. Karplus, Active-site dynamics in protein molecules – a stochastic boundary molecular-dynamics approach, Biopolymers 24 (1985) 843–865.
[32] M.R. Redinbo, L. Stewart, J.J. Champoux, W.G.J. Hol, Structural flexibility in human topoisomerase I revealed in multiple non-isomorphous crystal structures, Journal of Molecular Biology 292 (1999) 685–696.
[33] L. Stewart, G.C. Ireton, J.J. Champoux, The domain organization of human topoisomerase I, Journal of Biological Chemistry 271 (1996) 7602–7608.
[34] R. Depew, J. Wang, Conformational fluctuations of DNA helix, Proceedings of the National Academy of Sciences of the United States of America 72 (11) (1975) 4275–4279.
[35] H. Chen, Y. Liu, Z. Zhou, L. Hu, Z.-C. Ou-Yang, J. Yan, Temperature dependence of circular DNA topological states, Physical Review E 79 (4, Part 1) (2009), http://dx.doi.org/10.1103/PhysRevE.79.041926, ISSN 1539-3755.
[36] M. Lisby, J.R. Olesen, C. Skouboe, B.O. Krogh, T. Straub, F. Boege, S. Velmurugan, P.M. Martensen, A.H. Andersen, M. Jayaram, O. Westergaard, B.R. Knudsen, Residues within the N-terminal domain of human topoisomerase I play a direct role in relaxation, Journal of Biological Chemistry 276 (2001) 20220–20227.
[37] Y. Mo, C. Wang, W. Beck, A novel nuclear localization signal in human DNA topoisomerase I, Journal of Biological Chemistry 275 (52) (2000) 41107–41113, ISSN 0021-9258.
[38] P. Haluska, E. Rubin, A role for the amino terminus of human topoisomerase I, in: G. Weber, C.E.F. Weber (Eds.), Advances in Enzyme Regulation, vol. 38, 38th Symposium on Regulation of Enzyme Activity and Synthesis in Normal and Neoplastic Tissues, Indianapolis, Indiana, September 29–30, 1997, 1998, pp. 253–262, ISSN 0065-2571.
[39] L. Stewart, G. Ireton, J. Champoux, Reconstitution of human topoisomerase I by fragment complementation, Journal of Molecular Biology 269 (3) (1997) 355–372, ISSN 0022-2836.
[40] J. Alsner, J. Svejstrup, E. Kjeldsen, B. Sorensen, O. Westergaard, Identification of an N-terminal domain of eukaryotic DNA topoisomerase-I dispensable for catalytic activity but essential for in vivo function, Journal of Biological Chemistry 267 (18) (1992) 12408–12411, ISSN 0021-9258.
[41] K. Palle, L. Pattarello, M. van der Merwe, C. Losasso, P. Benedetti, M.-A. Bjornsti, Disulfide cross-links reveal conserved features of DNA topoisomerase I architecture and a role for the n terminus in clamp closure, Journal of Biological Chemistry 283 (41) (2008) 27767–27775, http://dx.doi.org/10.1074/jbc.M804826200, ISSN 0021-9258.
[42] G. Chillemi, M. Redinbo, A. Bruselles, A. Desideri, Role of the linker domain and the 203–214 N-terminal residues in the human topoisomerase I DNA complex dynamics, Biophysical Journal 87 (6) (2004) 4087–4097.